

**NASA
Technical
Memorandum**

NASA TM-86512

**DEVELOPMENT AND TEST OF ADVANCED
COMPOSITE COMPONENTS**

Center Director's Discretionary Fund Program

**By Gwyn Faile, Rose Hollis, Frank Ledbetter,
Juan Maldonado, Jim Sledd, Jim Stuckey,
Gerald Waggoner, and Erich Engler**

Structures and Propulsion Laboratory

June 1985



**(NASA-TM-86512) DEVELOPMENT AND TEST OF
ADVANCED COMPOSITE COMPONENTS. CENTER
DIRECTORS DISCRETIONARY FUND PROGRAM (NASA)
36 p HC A03/MF A01**

85-32147

CSCL 11D

**Unclas
21946**

G3/24



**National Aeronautics and
Space Administration**

George C. Marshall Space Flight Center

| | | | | | |
|---|--|--|--|---|-----------------------|
| 1. REPORT NO. NASA TM-86512 | | 2. GOVERNMENT ACCESSION NO. | | 3. RECIPIENT'S CATALOG NO. | |
| 4. TITLE AND SUBTITLE Development and Test of Advanced Composite Components Center Director's Discretionary Fund Program | | | | 5. REPORT DATE June 1985 | |
| | | | | 8. PERFORMING ORGANIZATION CODE | |
| 7. AUTHOR(S) G. Falle, R. Hollis, F. Ledbetter, J. Maldonado, J. Sledd, J. Stuckey, G. Waggoner, and E. Engler | | | | 8. PERFORMING ORGANIZATION REPORT # | |
| 9. PERFORMING ORGANIZATION NAME AND ADDRESS George C. Marshall Space Flight Center Marshall Space Flight Center, Alabama 35812 | | | | 10. WORK UNIT, NO. | |
| | | | | 11. CONTRACT OR GRANT NO. | |
| 12. SPONSORING AGENCY NAME AND ADDRESS National Aeronautics and Space Administration Washington, D.C. 20546 | | | | 13. TYPE OF REPORT & PERIOD COVERED Technical Memorandum | |
| | | | | 14. SPONSORING AGENCY CODE | |
| 15. SUPPLEMENTARY NOTES Prepared by Structures and Propulsion Laboratory, Science and Engineering. | | | | | |
| 16. ABSTRACT This report describes the design, analysis, fabrication, and test of a complex "bathtub fitting." Graphite fibers (P75) in an epoxy matrix were utilized in manufacturing of 11 components representing four different design and layup concepts. Design allowables were developed for use in the final stress analysis. Strain gage measurements were taken throughout the static load test and correlation of test and analysis data were performed, yielding good understanding of the material behavior and instrumentation requirements for future applications. | | | | | |
| 17. KEY WORDS Graphite Epoxy Composites Low CTE Components | | | 18. DISTRIBUTION STATEMENT Unclassified - Unlimited | | |
| 19. SECURITY CLASSIF. (of this report) Unclassified | | 20. SECURITY CLASSIF. (of this page) Unclassified | | 21. NO. OF PAGES 36 | 22. PRICE NTIS |

ACKNOWLEDGMENTS

A number of persons in various organizations had a significant role in the execution of this effort.

Personnel in the Structural Development Branch, Structures Engineering Branch, Polymers and Composites Branch, Structural Test Branch, Quality Control, and Developmental Sciences, Ontario, California, contributed to this task.

The authors offer their thanks to all contributors.

TABLE OF CONTENTS

| | Page |
|---------------------------------------|------|
| INTRODUCTION | 1 |
| COMPONENT DESIGN | 3 |
| MATERIAL CHARACTERIZATION | 8 |
| Equipment Used | 8 |
| Test Procedures | 8 |
| RESULTS AND DISCUSSION | 9 |
| Unidirectional Material | 9 |
| Quasi-Isotropic Material | 9 |
| STRUCTURAL ANALYSIS | 11 |
| COMPONENT FABRICATION | 11 |
| STRUCTURAL TEST | 14 |
| Summary | 14 |
| Test Description | 14 |
| Test Anomalies | 14 |
| Test Data | 14 |
| Test Results | 14 |
| CONCLUSIONS AND RECOMMENDATIONS | 29 |

LIST OF ILLUSTRATIONS

| Figure | Title | Page |
|--------|---|------|
| 1. | Focal Plane Structure (FPS) | 2 |
| 2. | Composite bathtub fitting | 3 |
| 3. | Fitting No. 1 (27M10003) | 4 |
| 4. | Fitting No. 2 (27M10001) | 5 |
| 5. | Fitting No. 3 (27M10002) | 6 |
| 6. | Fitting No. 4 (21M21009) | 7 |
| 7. | Bathtub fitting finite element model | 12 |
| 8. | Bathtub fitting in a composite structural test setup (view 1) | 16 |
| 9. | Bathtub fitting in a composite structural test setup (view 3) | 17 |
| 10. | Bathtub fitting mounting anomaly for Specimen 27M10003 SN1 | 18 |
| 11. | Strain gage and failure locations | 20 |
| 12. | Strain gage and failure locations | 23 |
| 13. | Strain gage and failure locations | 26 |
| 14. | Strain gage locations | 29 |
| 15. | Progressive failure analysis | 30 |

LIST OF TABLES

| Table | Title | Page |
|-------|--|------|
| 1. | Properties of Unidirectional P75S/934 | 10 |
| 2. | Properties of (0/±45/90) _{ns} P75S/934 | 10 |
| 3. | Comparison of Elastic Properties for (0/±45/90) _{ns} P75S/934, Predicted Versus Measured | 11 |
| 4. | Process and Cure Cycle Summary for DSI Part for NASA Drawing Number 27M10003-1 | 13 |
| 5. | Test Results | 15 |
| 6. | 27M10001 S/N2 Strain Gage Test Data | 19 |
| 7. | 27M10001 Strain Gage Test Data | 19 |
| 8. | 27M10001 Strain Gage Test Data | 20 |
| 9. | 27M10002 Strain Gage Test Data | 21 |
| 10. | 27M10002 Strain Gage Test Data | 21 |
| 11. | 27M10002 Strain Gage Test Data | 22 |
| 12. | 27M10002 Comparison of Tests and SQ5 Results | 22 |
| 13. | 27M10002 Comparisor of Test and SQ5 Results | 23 |
| 14. | 27M10003 Strain Gage Test Data | 24 |
| 15. | 27M10003 Strain Gage Test Data | 24 |
| 16. | 27M10003 Strain Gage Test Data | 25 |
| 17. | 27M10003 Comparison of Test and SQ5 Results | 25 |
| 18. | 27M10003 Comparison of Test and SQ5 Results | 26 |
| 19. | 27M10009 Strain Gage Test Data | 27 |
| 20. | 27M10009 Strain Gage Test Data | 27 |
| 21. | 27M10009 Strain Gage Test Data | 28 |
| 22. | 27M10009 Comparison of Test and SQ5 Results | 28 |
| 23. | 27M10009 Comparison of Test and SQ5 Results | 28 |

TECHNICAL MEMORANDUM

DEVELOPMENT AND TEST OF ADVANCED COMPOSITE COMPONENTS

INTRODUCTION

The report documents the development effort to improve the design and load-carrying ability of a complex corner fitting, using advanced filament composites in a resin matrix (Epoxy).

The Optical Telescope Assembly portion of the Space Telescope contains a number of graphite epoxy structures. One of these structures is the Focal Plane Structure (FPS) (Fig. 1), a critical structural assembly requiring a high order of thermal stability, structural stiffness, and low weight. The graphite epoxy layup of the FPS is designed to achieve a coefficient of thermal expansion (CTE) of $\pm 0.09 \times 10^{-6}$ in./in./°F. Among the components making up the FPS are eight brackets that provide support for the four radial instruments that are carried on the FPS. These eight brackets are of a configuration commonly known as "bathtub fittings" in aerospace structures parlance, and are of titanium.

The original design of these bathtub fittings, however, was of graphite epoxy with a pseudoisotropic layup to achieve the specified CTE. Structural testing of these bathtub fittings to 1.4 x limit load was required to verify the design. These fittings failed in test, some demonstrating an ultimate factor-of-safety of only 1.15 instead of the required 1.4 factor.

Due primarily to these unpredicted low factors (schedule was also an important deciding factor), the penalties in weight and pointing stability were accepted and the fittings were redesigned for titanium. As a number of new projects, such as AXAF, require optical benches with stringent dimensional stability during thermal excursion, application of graphite/epoxy composites will be required.

Existing technology is limited in design, analysis, fabrication, and test of complex components, fabricated from Pitch 75 graphite fibers, especially the effects of layup changes on the ultimate strength, the stress distribution and correlation of strain gage data to analysis results.

Since bathtub fittings are a common configuration for aerospace structures, it became obvious that development work for such fittings is required if graphite epoxy is to be a viable candidate for these structures.

The development objectives for this program were: evaluation of layup changes to improve ultimate strength of fabricated components, develop basic material data, establish analysis methods, and verify the design and analysis through test of full-size components.

In order to eliminate erroneous results, it was decided to fabricate and test three parts of each design. This would average the variations in as-fabricated properties and tolerances.

ORIGINAL PAGE IS
OF POOR QUALITY

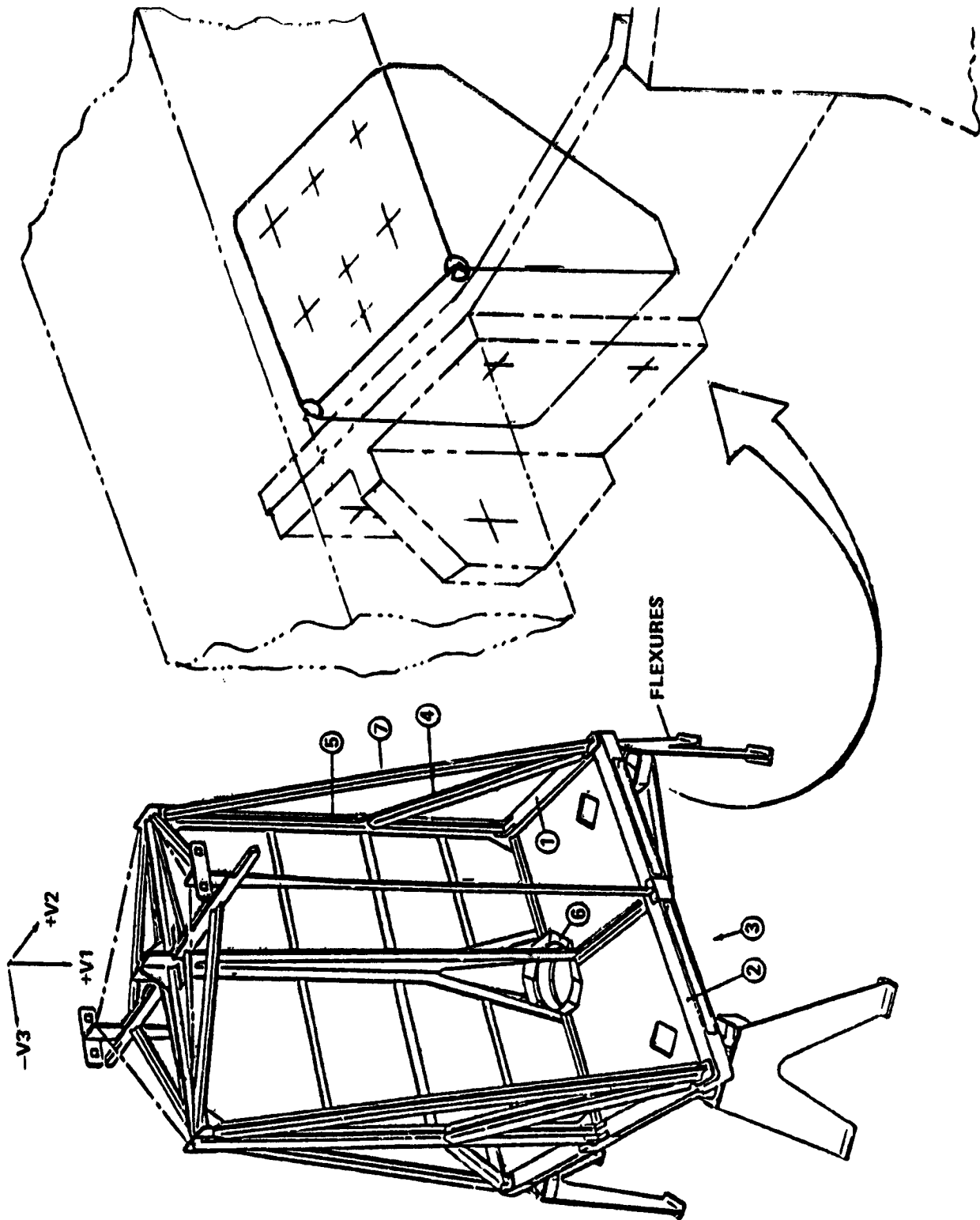


Figure 1. Focal Plane Structure (FPS).

COMPONENT DESIGN

The component selected for the development effort has a complex shape, referred to as "bathtub fitting," and is shown in Figure 2. Four different designs were executed, differing from each other by the arrangement (layup) of the composite material. Designs are shown on Figures 3 through 6.

Analysis of the failed initial FPS bathtub fitting showed that the fractures developed along the laminate splice-lines. Due to the laminate flat pattern designs, these splice-lines lay along the corners of the fittings and had only a slight stagger between plies. The three layup patterns selected for this program were designed maintaining the same laminate material, fiber orientation, resin content, and basic dimensions of the P-E fittings. However, the layup patterns were modified to relocate the splice-lines in planes away from the corners. Also, radius fillers were added for the areas in contact with the test fixture and bolt heads.

The following discussion summarizes the design variations. Figure 2 details the basic dimensions, the radius fillers, and the alternating of the laminate flat patterns. Figure 3 shows the first design (27M1003) which is the original FPS bathtub fitting. Additional fittings of this design were fabricated to compare their fabrication quality to the originals — to minimize test errors due to variation in workmanship. Figure 4 gives another layup (27M1001) which relocated the splice-lines to the sides of the fitting with staggered splice-line angles of 30 deg and 60 deg. The third design, Figure 5 (27M10002), had overlapping "tabs" on the top and back planes so that each laminate had one continuous (not spliced) surface for each surface that was spliced. These additional tabs increased the wall thickness on these surfaces but afforded better continuity. The last design, Figure 6 (21M10009), is an assembly of three laminates, each of which provided continuity around the corners in one direction (a total of three laminates for the three viewing axis). Reduced drawings for all components are attached to the report.

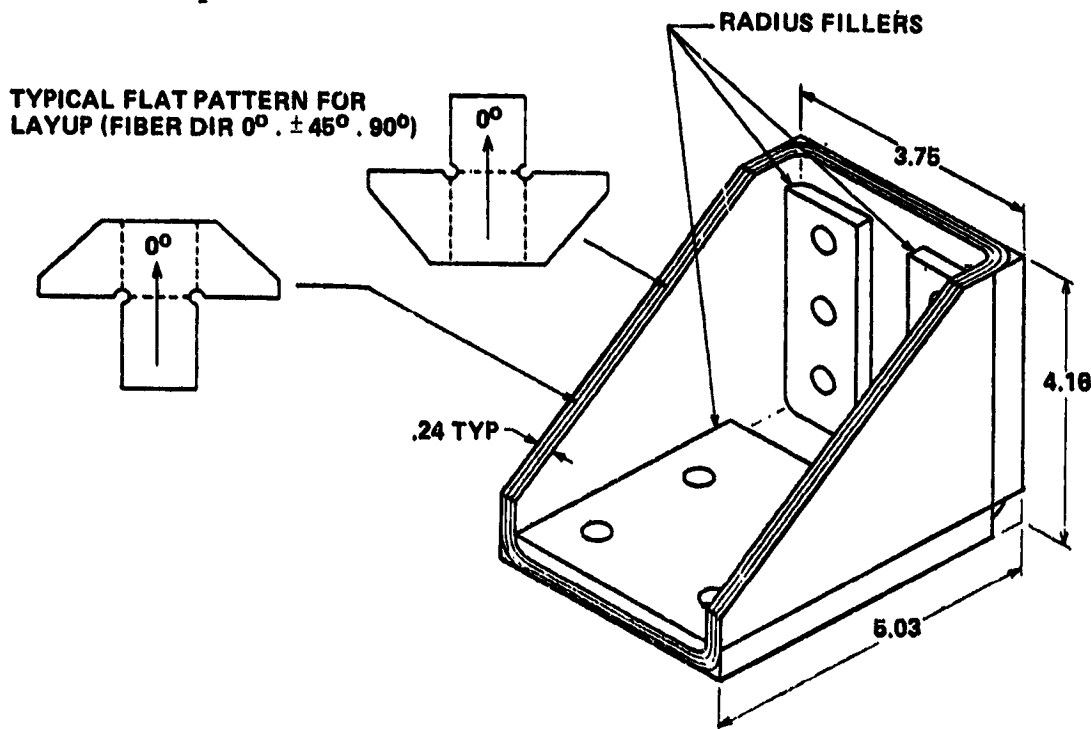
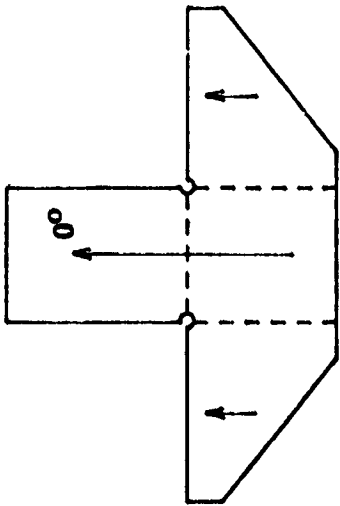
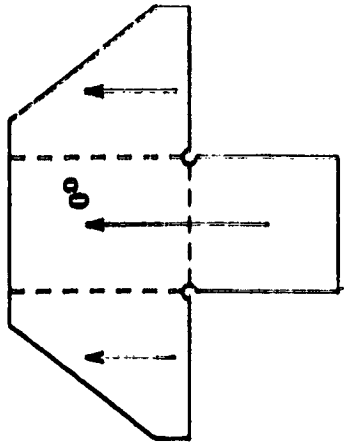
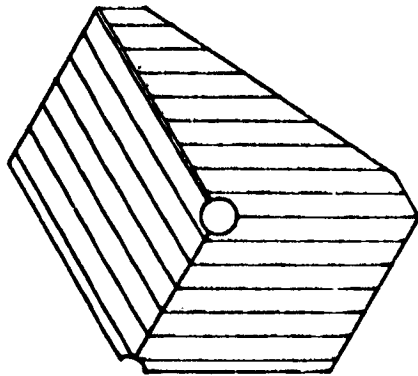


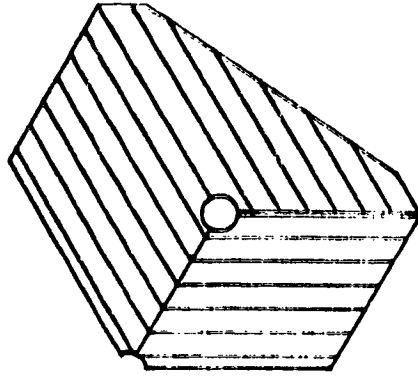
Figure 2. Composite bathtub fitting.



FLAT PATTERN I

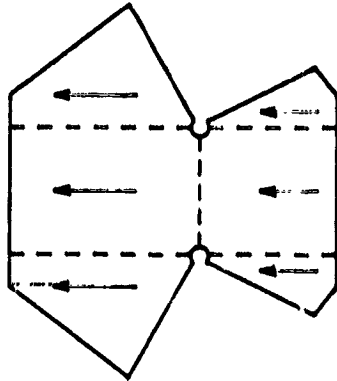


FLAT PATTERN II

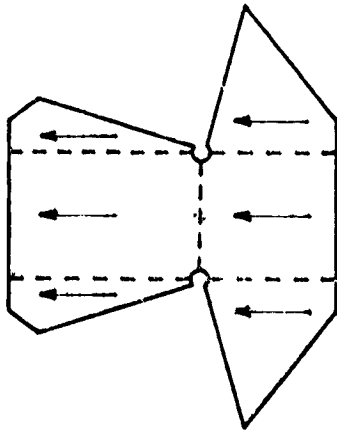
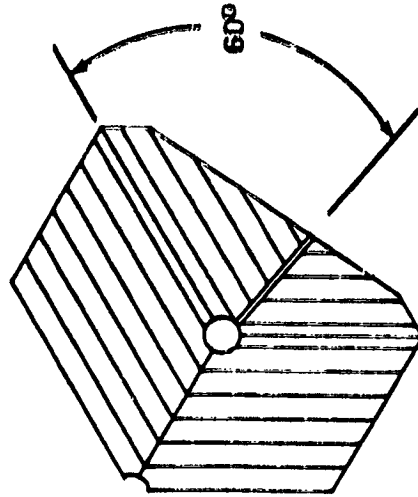


AS LAID-UP ON FITTING

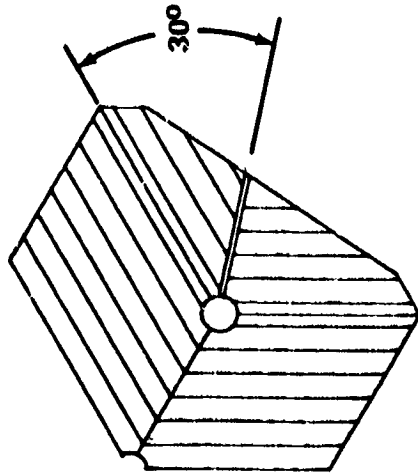
Figure 3. Fitting No. 1 (27M10003).



FLAT PATTERN II

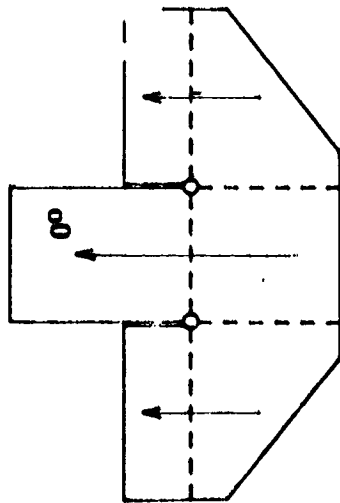


FLAT PATTERN I

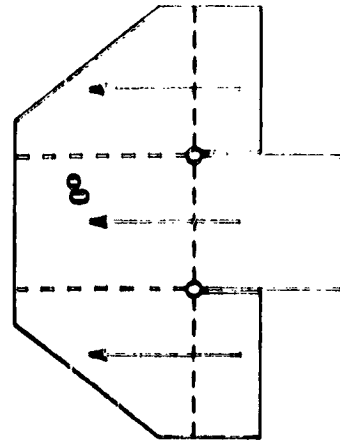
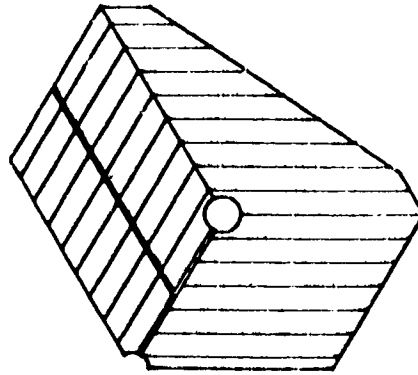


AS LAID-UP ON FITTING

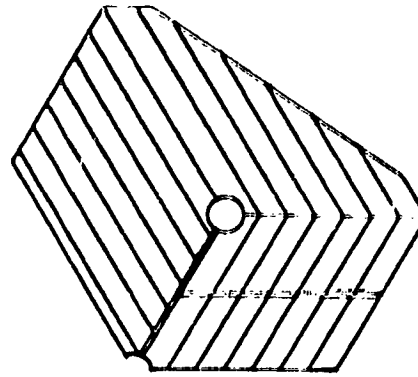
Figure 4. Fitting No. 2 (27M10001).



FLAT PATTERN I



FLAT PATTERN II



AS LAID-UP ON FITTING

Figure 5. Fitting No. 3 (27M10002).

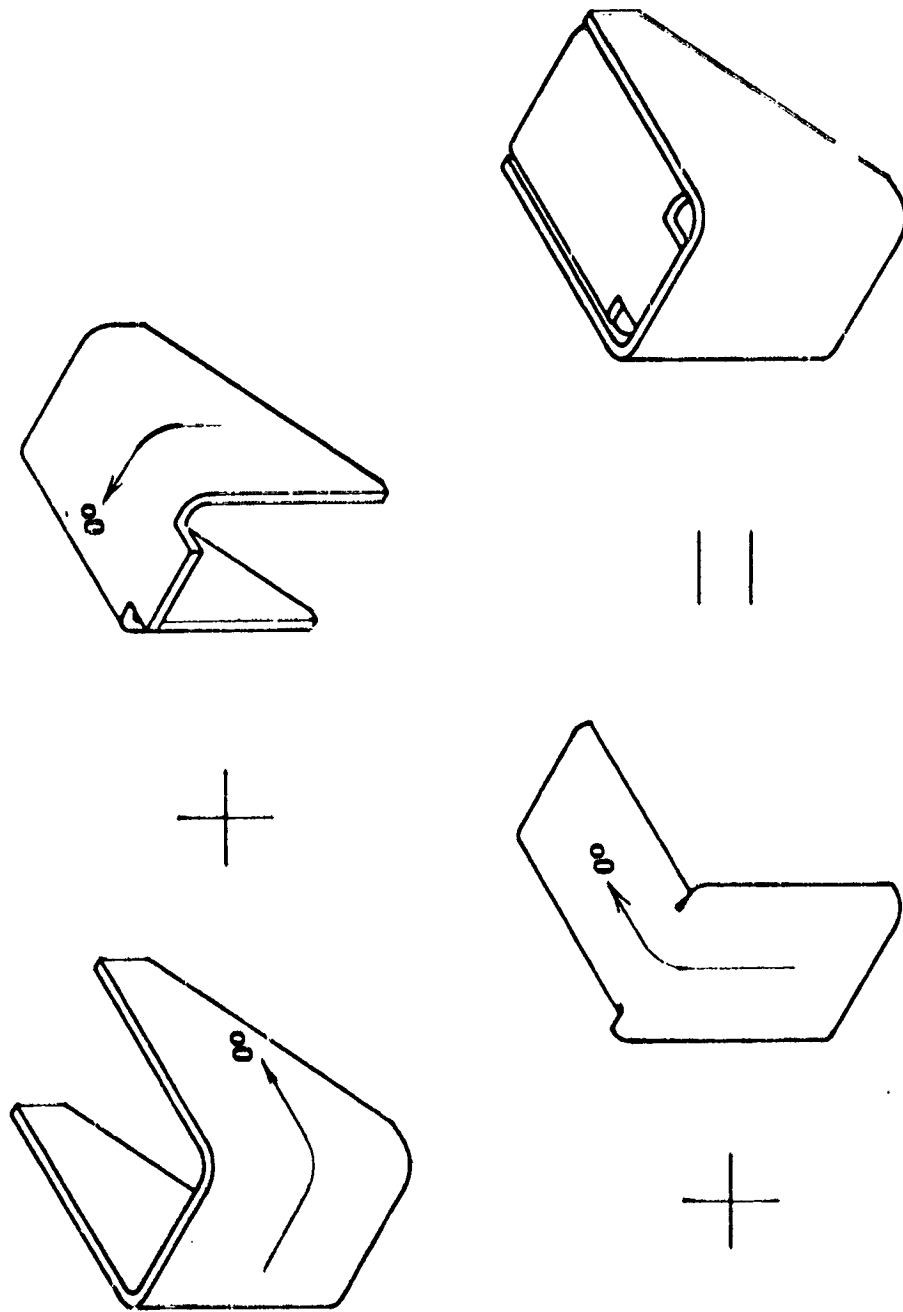


Figure 6. Fitting No. (31M21009).

MATERIAL CHARACTERIZATION

The P75S/934 graphite/epoxy bathtub fittings were modeled using the finite element method in order to predict their behavior under actual loading conditions. For the model to be somewhat accurate, material properties of the system had to be determined. The material properties determined for this system include tensile, compressive, and shear properties for both unidirectional and quasi-isotropic (0/±45/90) laminates.

Equipment Used

The P75S/934 tape was supplied by Fiberite, Inc., to Developmental Sciences, Inc., which then prepared laminates and supplied them to the Marshall Space Flight Center for characterization. The laminates were cut into the desired sample sizes by a water-cooled diamond saw, and holes were drilled in the laminates (when appropriate) by a water-cooled drill press. An Instron 1125 mechanical testing machine, in conjunction with a Fluke 2450 MCS data acquisition system, was used to determine the mechanical properties of the material. Fiber volume fractions were obtained by determining the density of the composite material and then, assuming no voids were present, comparing that density with the reported densities for the fiber and resin as supplied by Fiberite to determine the fiber volume fraction.

Test Procedures

Unidirectional Material

Tensile tests were performed on unidirectional material to determine longitudinal and transverse Young's Moduli, E_1 and E_2 , longitudinal and transverse ultimate strengths, F_0^{tu} and F_{90}^{tu} , and the major Poisson's ratio ν_{12} . The tests were performed according to ASTM D3039-76. 8-ply laminates with specimen dimensions 0.500 in. wide by 9.00 in. long, using a 6.00-in. gage length, were used to determine E_1 , F_0^{tu} , and ν_{12} ; 16-ply laminates, with specimen dimensions 1.000 in. wide by 6.50 in. long, using a 3.50-in. gage length, were used to determine E_2 and F_{90}^{tu} .

Compression tests were performed to determine F_0^{cu} and F_{90}^{cu} , the longitudinal and transverse compressive strengths, respectively. The test method used was ASTM D3410-75 (the Cleanese test fixture). 16-ply laminates, with specimen dimensions 0.250 in. wide by 5.5 in. long, using a 0.500-in. gage length, were used to determine both F_0^{cu} and F_{90}^{cu} .

In-plane shear tests were performed to determine the inplane shear modulus G_{12} in the inplane shear strength F^{su} . Two different tests were used to determine these properties. G_{12} was determined by the three-rail shear test (in ASTM, committee, not published), and F^{su} was determined by the 45 deg off-axis tensile test (same procedure as ASTM D3039-76). 16-ply laminates were used for both procedures; sample

dimensions were 6.00 in. by 6.00 in. with nine approximately spaced 0.5-in. diameter holes for the rail shear test and 1.00 in. wide by 9.00 in. long with a 6.00-in. gage length for the 45 deg off-axis test.

Quasi-Isotropic Material

Tensile tests on quasi-isotropic material were performed to determine E_x , $F_x^{t.u}$, and ν_{xy} , the longitudinal (and transverse) Young's Modulus, ultimate tensile strength, and Poisson's ratio, respectively. 16-ply laminates ($0/\pm 45/90_{2S}$) and 24-ply laminates ($0/\pm 45/90_{3S}$) were both used for comparative purposes. Sample dimensions were identical to those for the 90 deg tensile tests.

Compression tests were used to determine F_c^{cu} , the longitudinal (and transverse) compressive strength. 16-ply laminates were used, and sample dimensions were identical to those used on unidirectional material.

Three-rail shear tests were used to determine the inplane shear modulus and shear strength, G_{xy} and F^{su} . Both 16-ply and 24-ply laminates were used, and specimen dimensions were identical to those for the unidirectional material.

RESULTS AND DISCUSSION

The material properties that were determined agree well with those obtained in other laboratories for the same material. All properties may be found in Tables 1 and 2, including fiber volume fractions.

Unidirectional Material

Based on the fiber volume fraction and the given properties for the P75S fibers, the results for the unidirectional material seem reasonable, allowing for discrepancies in the determination of the fiber volume fraction.

One problem that did occur in the characterization of the unidirectional material was obtaining a representative inplane shear strength. The rail shear test results in very low shear strengths for unidirectional material, so the 45 deg off-axis tensile test was used to determine shear strength. However, the strengths that are obtained by this method can be as much as 30 to 40 percent low. Thus, the values obtained may be very conservative.

Quasi-Isotropic Material

Elastic properties (E_x , ν_{xy} , G_{xy}) for quasi-isotropic material can be predicted, based on unidirectional properties, by the use of classical lamination theory (CLT). The properties that were measured could be compared with those that were predicted.

The Young's Modulus obtained for 16-ply laminates agreed well with that predicted by CLT; however, the Poisson's ratio and inplane shear modulus did not. The Poisson's ratio was not good, probably because of poor strain gages, and the shear modulus was not good because of testing problems. Because of a lack of any more 16-ply material, 24-ply materials were tested to obtain better results.

TABLE 1. PROPERTIES OF UNIDIRECTIONAL P75S/934

| | | V_f |
|---------------------|-------|-------|
| E_1 , Msi | 39.2 | 0.56 |
| E_2 , Msi | 1.14 | 0.60 |
| G_{12} , Msi | 0.574 | 0.60 |
| ν_{12} , Msi | 0.337 | 0.56 |
| F_0^{tu} , ksi | 105.5 | --- |
| F_0^{cu} , ksi | 42.0 | --- |
| F_{90}^{tu} , ksi | 3.03 | --- |
| F_{90}^{cu} , ksi | 15.8 | --- |
| F^{su} , ksi | 3.02 | --- |

TABLE 2. PROPERTIES OF $(0/\pm 45/90)_{ns}$ P75S/934

| | | <u>No. of Plies</u> | V_f |
|------------------|-------|---------------------|-------|
| E_x , Msi | 14.6 | 16 | 0.57 |
| G_{xy} , Msi | 5.16 | 24 | 0.58 |
| ν_{xy} | 0.343 | 24 | 0.58 |
| F_x^{tu} , ksi | 39.4 | 16 | --- |
| F_x^{cu} , ksi | 28.0 | 16 | --- |
| F^{cu} , ksi | 5.62 | 16 | --- |

The Poisson's ratio and inplane shear modulus agreed with theory for the 24-ply material, but the Young's modulus did not. One inference that may be made is that the Young's modulus may be thickness-dependent, while the other two elastic properties may or may not be dependent on thickness. Table 3 compares CLT values with the actual measured values for the material.

Although strength properties cannot be predicted by CLT, the results were within reason for a quasi-isotropic laminate, compared to the unidirectional properties.

The inplane shear strength may again be too conservative, and is based on the 16-ply tests because the loads required on the 24-ply samples were so great that the samples slipped in the test fixture. --

TABLE 3. COMPARISON OF ELASTIC PROPERTIES FOR (0/±45/90)_{ns}
P75S/934, PREDICTED VERSUS MEASURED

| | <u>Predicted</u> | <u>Measured</u> | |
|----------------|------------------|--------------------|-----------------|
| | | <u>16 Plies</u> | <u>24 Plies</u> |
| E_x , Msi | 13.9 | 14.6 | 11.4 |
| G_{xy} , Msi | 5.25 | 4.30 ^a | 5.16 |
| ν_{xy} | 0.325 | 0.376 ^b | 0.343 |

- a. Slippage in fixture and possible strain gage bonding problems.
- b. Possible strain gage bonding problems.

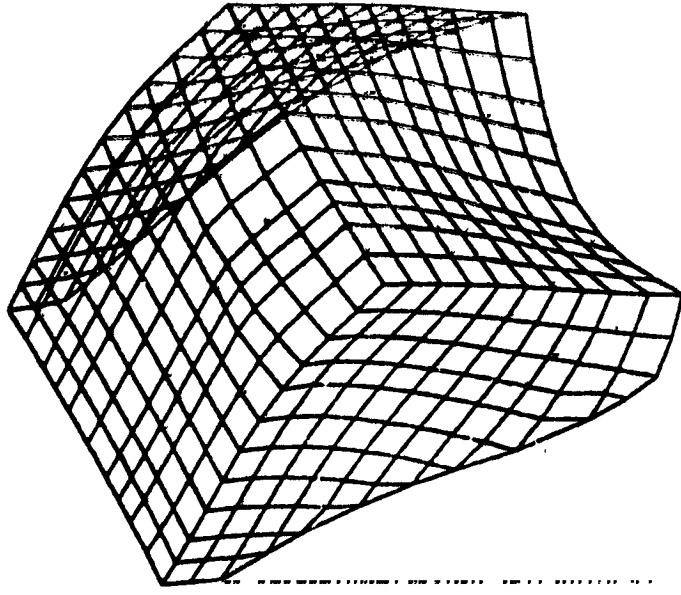
STRUCTURAL ANALYSIS

The finite element method and classical lamination theory were used to perform the analysis. A finite element program (SPAR) was used in an uncoupled format to calculate laminate in-plane force resultants (N_x , N_y , N_{xy}) and moment resultants (M_x , M_y , M_{xy}). These were then input into a laminate point stress analysis program (SQ5) to calculate surface strains, which were compared with test strain gage data. The finite element model is present in Figure 7.

COMPONENT FABRICATION

The composite components were fabricated under contract by Development Sciences, Inc., 15757 E. Valley Boulevard, P.O. Box 1264, City of Industry, California 91749. Also included were the production of the flat panels needed for material characterization samples. The individual layers were cut according to the template pattern and laid up on a male steel mold with approximately 1 in. excess for trimming to final dimensions. A precompaction operation was performed after every eight plies to eliminate voids and wrinkles (Table 4). The prepreg used was P75/934, supplied by Fiberite Corporation, and the parts were processed as shown on Table 4, including the bonding operation required for parts 21M1009. The ply orientations were inspected during layup and before bagging of the completed part. After curing, the holes were drilled and final contour machined. Similar inspection was required for the flat panels. Shipping inspection at the contractor plant, including dimensional verification or deviation documentation, was performed. At MSFC, the parts were inspected for dimensional conformance and overall appearance.

DEFORMED AFTER LOADING



UNDEFORMED PRIOR TO LOADING

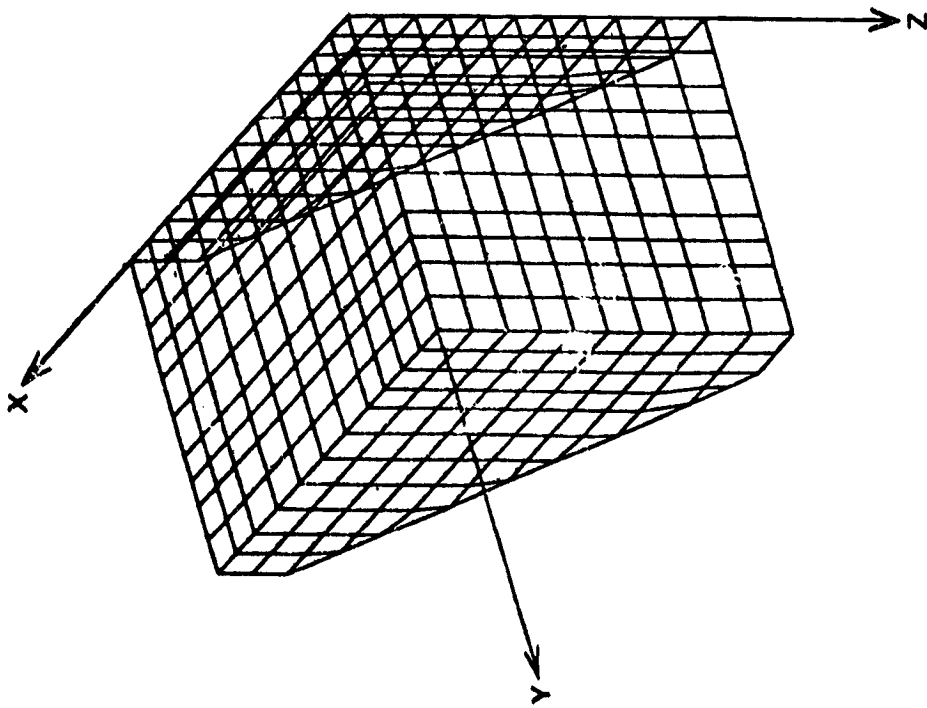


Figure 7. Bathtub fitting finite element model.

TABLE 4. PROCESS AND CURE CYCLE SUMMARY FOR
DSI PART FOR NASA DRAWING NUMBER 27M10003-1

1. Pre-compaction - every 8 plies @ 150°F and 7 psi (vacuum only) 1.0 hr.
2. Cure
 1. Place in A/C draw full vacuum (26 ± 2 " Hg)
 2. Pressurize to 100 ± 5 psig - vent vacuum to atmosphere @ 25 psig
 3. Ramp Heat-up @ $2-5^\circ\text{F}/\text{min}$ to $250^\circ\text{F} \pm 10^\circ\text{F}$
 4. Hold 250°F 60 min.
 5. Ramp Heat-up @ $2-5^\circ\text{F}/\text{min}$ to $350^\circ\text{F} \pm 10^\circ\text{F}$
 6. Hold 350°F 120 min.
 7. Cool down under pressure @ $2 \pm 1^\circ\text{F}/\text{min}$ to 150°F max.
 8. Release pressure and remove from A/C.
3. Bond and Post Cure
 1. Apply *EA934 to all faying surfaces - apply mechanical pressure to ≈ 20 psi
 2. Place in air convected oven
 3. Heat-up @ $2-5^\circ\text{F}/\text{min}$ to $150^\circ\text{F} \pm 10^\circ\text{F}$
 4. Hold 30 min @ 150°F
 5. Heat-up @ $2-5^\circ/\text{min}$ to $250^\circ\text{F} \pm 10^\circ\text{F}$
 6. Hold 30 min @ 250°F
 7. Heat-up @ $2-5^\circ\text{F}/\text{min}$ to $350^\circ\text{F} \pm 10^\circ\text{F}$
 8. Hold 480 min (8 hrs) @ 350°F
 9. Cool Down @ $2^\circ \pm 1^\circ\text{F}$ to 150°F
 10. Remove from oven.

Cure charts available for pre-compaction and cure.

*EA934 is an asbestos filled adhesive per the included data sheets 1 through 3.

Results

Inspection of delivered parts at MSFC revealed the following: all thicknesses, which are determined by the number of plies, were approximately 20 percent above the the specified dimensions on the drawings. The discrepancy was traced to the fact that the contractor had ordered a prepreg material with a Fiber Area Weight (FAW) of $159 \text{ gr}/\text{m}^2$ with a resin content of 37 percent by weight. In order to achieve a nominal cured layer thickness of 0.005 in., the required FAW would be $142 \text{ g}/\text{m}^2$. As the contractor had used the material with the higher FAW and complied with the prescribed resin content (37 percent by weight), the ply thickness increased to 0.0062 and all dimensions depending on the number of layers increased accordingly. This change was accounted for in the analysis and material property documentation. Furthermore, due to the layup on a male mandrel, the interfaces to the test fixtures were not always flat and some shimming was required.

STRUCTURAL TEST

Summary

The composite material "bathtub" fittings were loaded to failure during the period of November 7, 1984, to July 10, 1984. The ultimate failure load varied from a low of 2,229 lb to a high of 4,492 lb. Table 5 gives a listing of the test specimen and the ultimate failure load.

Test Description

Each "bathtub" fitting was instrumented with strain gages as per requirements of the stress analyst. The component was then installed into the test setup (Fig. 8 and 9) with mechanical measurements to verify the alignment. Two deflection gages were utilized, one to monitor movement/deflection of the support structure and one to monitor the deflection of the "bathtub" fitting.

The loading sequence for the first test specimen was as follows: (a) compressive load of 1,000 lb and return to zero; and (b) tension load until failure. All succeeding specimen were loaded to 1,000 lb tension (increments of 250 lb) then returned to zero. The procedure was repeated until an acceptable repeat of zero was obtained. A tension load was then applied until the test specimen failed. The load, deflection, and strains were recorded, beginning prior to start of loading and ending after test specimen failure, at a rate of 1 scan per 200 msec.

Test Anomalies

The test specimen, 27M10003 SN-1 did not have fillet inserts. When the specimen was installed into the test fixture, there were gaps between the specimen and the test fixture. The procedure used for attaching the specimen was as follows: the two lower bolts were torqued first, then the two top bolts. After torquing, the gaps between the specimen and the mounting surface were measured. Figure 10 illustrates the condition that existed.

The deflection gages were inoperative during the testing of specimens 6, 7, 8, and 9. This was the result of an equipment malfunction that was not detected until test preparation for specimen 10.

Test Data

A printout of all test data was furnished at the completion of the test for each specimen. The data tapes will be retained for a period of one year.

Test Results

Table 5 presents the ultimate failure loads. The results for each group of fittings are presented in the following four sections.

TABLE 5. TEST RESULTS

| <u>Bathtub Fitting</u> | <u>Date Tested</u> | <u>Ultimate Failure Load (lbs)</u> |
|------------------------|--------------------|------------------------------------|
| 27M10001 S/N3 | 11-4-83 | 4046 |
| 27M10001 S/N4 | 2-14-84 | 3703 |
| 27M10001 S/N2 | 5-17-84 | 3492 |
| 27M10002 S/N2 | 6-20-84 | 4492 |
| 27M10002 S/N4 | 6-21-84 | 4083 |
| 27M10002 S/N3 | 7-9-84 | 4387 |
| 27M10003 S/N1 | 7-9-84 | 2229* |
| 27M10003 S/N2 | 7-9-84 | 3266 |
| 27M10003 S/N3 | 7-9-84 | 3659 |
| 27M10009 S/N2 | 7-10-84 | 3237 |
| 27M10009 S/N1 | 7-10-84 | 3015 |

* Did not have radius insert.

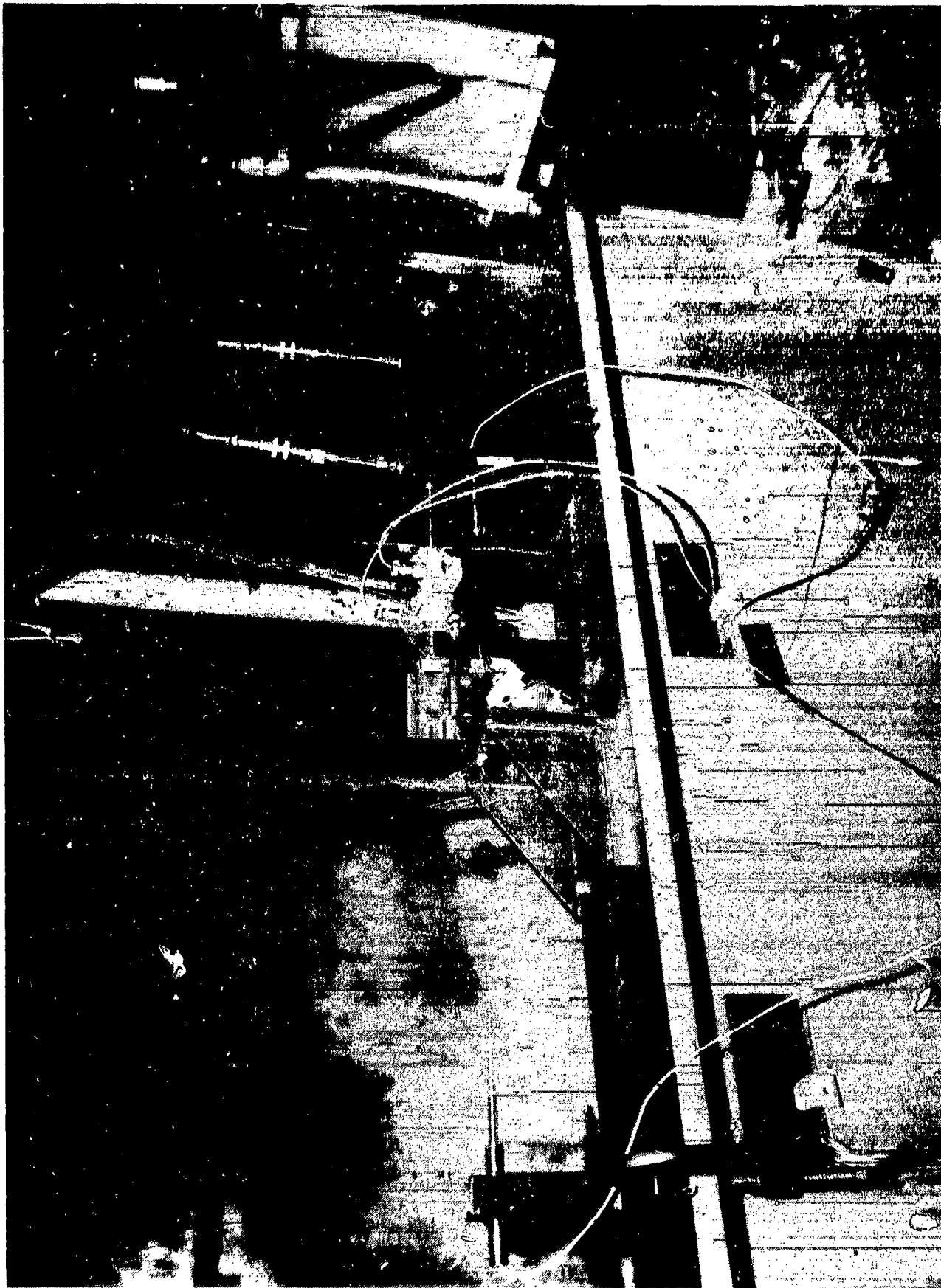


Figure 8. Bathtub fitting in a composite structural test setup (view 1).

ORIGINAL FACED
OF POOR QUALITY



Figure 9. Bathtub fitting in a composite structural test setup (view 3).

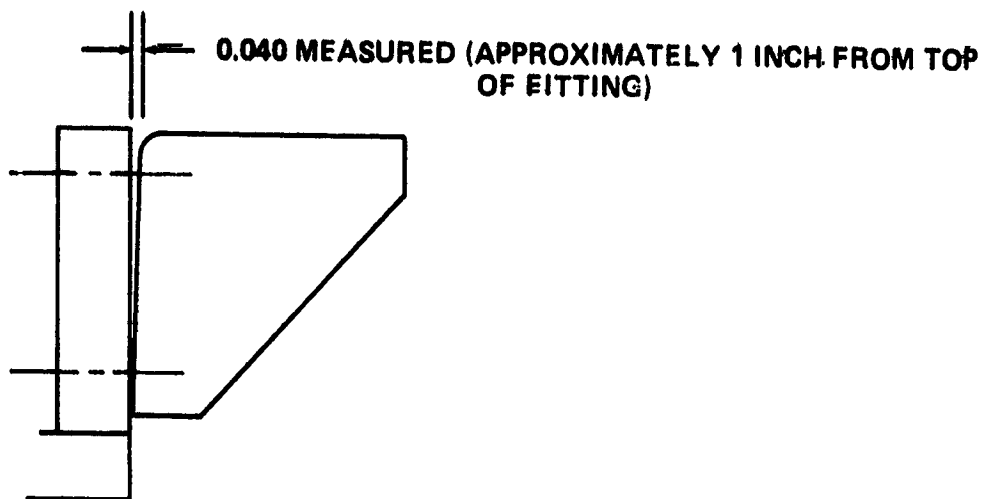
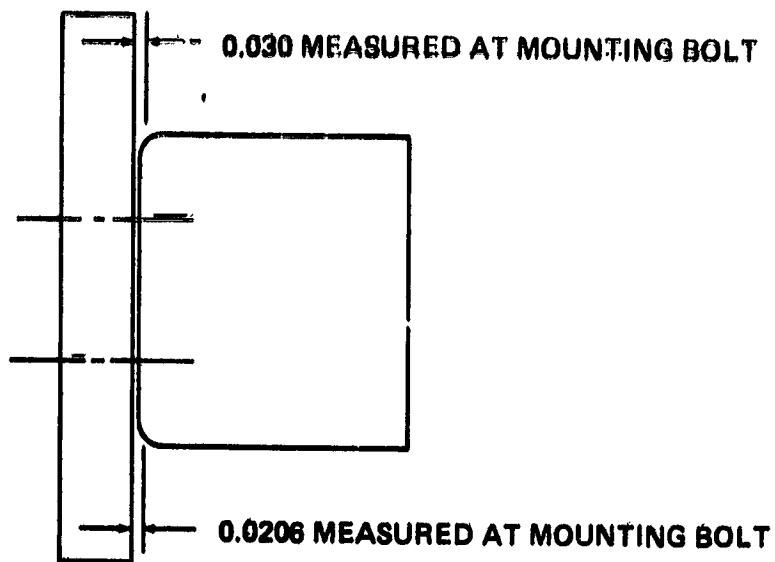


Figure 10. Bathtub fitting mounting anomaly for Specimen 27M10003 SN1.

1. 27M10001 Test Results

There was a problem with the kapton backing used for the first test, S/N 3, and 66 percent of the 82 channels did not provide data suitable for evaluation purposes. Kapton was not used on any of the following tests, and the number of channels was reduced to 39 for S/N2 and S/N4. Channels 1T13 and 3T13 were lost on S/N2, and channel 1T13 was lost on S/N4. Also, other strain gage locations were not optimal. They were located either too close to free edges or too close to the seams of the laminate layup. Data for three of those locations are presented in Tables 6 through 8. Location of those strain gages is presented on Figure 11. On the remaining fittings, it was decided to reduce the number of channels to 9 (3 rosettes) and to place the strain gages in locations where failures occurred.

TABLE 6. 27M10001 S/N2 STRAIN GAGE TEST DATA (μ in./in.)

| <u>Load (lb)</u> | <u>3T1</u> | <u>3T2</u> | <u>3T3</u> | <u>12T1</u> | <u>12T2</u> | <u>12T3</u> |
|------------------|------------|------------|------------|-------------|-------------|-------------|
| 0 | 6 | 3 | 3 | 3 | 3 | 6 |
| 276 | 24 | 43 | -3 | 33 | -12 | 12 |
| 505 | 43 | 66 | 6 | 55 | -24 | 21 |
| 1105 | 85 | 143 | -12 | 118 | -58 | 48 |
| 1536 | 106 | 203 | -12 | 161 | -82 | 73 |
| 1960 | 137 | 270 | -12 | 197 | -106 | 100 |
| 2492 | 155 | 385 | -3 | 221 | -130 | 139 |
| 2994 | 161 | 498 | -21 | 215 | -143 | 160 |

These are strain gages in the same location on opposite sites of the fitting. (Refer to Figure 11.)

TABLE 7. 27M10001 STRAIN GAGE TEST DATA (μ in./in.)

| <u>Loads (lb)</u> | <u>S/N4</u> | | | <u>S/N2</u> | | | <u>S/N4</u> | | | <u>S/N2</u> | | |
|-------------------|-------------|------------|------------|-------------|------------|------------|-------------|------------|------------|-------------|------------|------------|
| | <u>7T1</u> | <u>7T2</u> | <u>7T3</u> | <u>7T1</u> | <u>7T2</u> | <u>7T3</u> | <u>8T1</u> | <u>8T2</u> | <u>8T3</u> | <u>8T1</u> | <u>8T2</u> | <u>8T3</u> |
| 0 | -6 | -3 | -3 | 3 | 3 | 3 | -3 | 0 | -3 | 3 | 3 | 3 |
| 242 | 3 | -3 | 3 | -6 | 6 | -12 | 19 | -3 | -80 | 52 | -3 | -6 |
| 529 | 10 | -3 | 13 | -23 | 6 | -30 | 51 | -3 | -170 | 103 | -12 | -18 |
| 1045 | 26 | -3 | 26 | -49 | 9 | -61 | 99 | -6 | -330 | 203 | -31 | -42 |
| 1505 | 45 | -6 | 42 | -103 | 18 | -94 | 151 | -6 | -487 | 334 | -67 | -79 |
| 2010 | 67 | -10 | 54 | -155 | 33 | -128 | 212 | -10 | -673 | 455 | -116 | -115 |
| 2519 | 90 | -16 | 71 | -325 | 103 | -94 | 276 | -6 | -868 | 713 | -186 | -191 |
| 3031 | 128 | -19 | 90 | -547 | 131 | -97 | 386 | 0 | -1140 | 989 | -204 | -240 |

These are strain gages in the same location on two different fittings with the same design. (Refer to Figure 11.)

TABLE 8. 27M10001 STRAIN GAGE TEST DATA ($\mu\text{in./in.}$)

| Loads (lb) | S/N4 | | | S/N2 | | | S/N4 | | | S/N2 | | |
|------------|------|-----|-----|------|-----|-----|------|------|------|------|------|------|
| | 9T1 | 9T2 | 9T3 | 9T1 | 9T2 | 9T3 | 10T1 | 10T2 | 10T3 | 10T1 | 10T2 | 10T3 |
| 0 | -3 | -3 | -10 | 3 | 0 | 3 | -3 | -3 | -3 | 3 | 0 | 3 |
| 242 | 48 | 29 | -10 | 21 | 24 | 12 | -10 | -20 | -20 | -40 | -37 | 3 |
| 529 | 110 | 64 | -10 | 46 | 48 | 24 | -20 | -50 | -61 | -103 | -70 | 0 |
| 1045 | 219 | 135 | -23 | 85 | 91 | 42 | -48 | -103 | -119 | -209 | -152 | 0 |
| 1505 | 319 | 200 | -23 | 124 | 133 | 61 | -64 | -158 | -190 | -297 | -238 | 3 |
| 2010 | 422 | 271 | -23 | 176 | 181 | 76 | -77 | -213 | -267 | -384 | -326 | -9 |
| 2519 | 510 | 338 | -13 | 155 | 209 | 112 | -77 | -261 | -354 | -340 | -342 | -64 |
| 3031 | 522 | 383 | 42 | 36 | 148 | 118 | -90 | -325 | -425 | -161 | -299 | -112 |

These are strain gages in the same location on two different fittings with the same design. (Refer to Figure 11.)

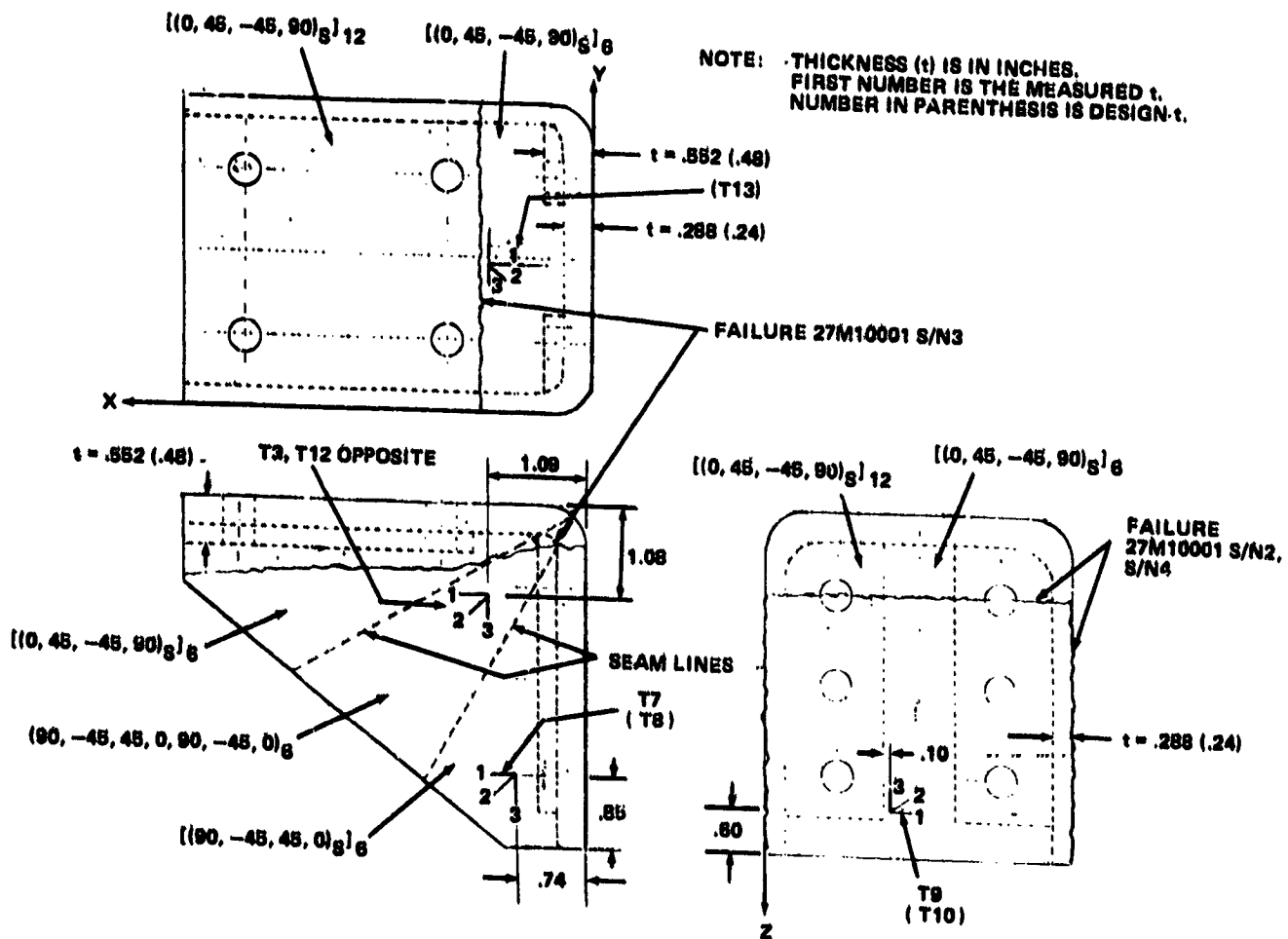


Figure 11. Strain gage and failure locations.

2. 2710002 Test Results

Tables 9 through 11 present strain gage test data. Tables 12 and 13 present comparison of test and analytical results. Locations of strain gages are presented on Figure 12. The three fittings failed across the bolt holes on the x-face at an average load of 4321 lb. This was the highest average failure load of all four test configurations.

TABLE 9. 27M10002 STRAIN GAGE TEST DATA (μ in./in.)

| <u>Load (lb)</u> | 1T13 | | | 2T13 | | | 3T13 | | |
|------------------|-------------|-------------|-------------|-------------|-------------|-------------|-------------|-------------|-------------|
| | <u>S/N2</u> | <u>S/N3</u> | <u>S/N4</u> | <u>S/N2</u> | <u>S/N3</u> | <u>S/N4</u> | <u>S/N2</u> | <u>S/N3</u> | <u>S/N4</u> |
| 500 | 134 | 143 | 149 | 58 | 39 | 01 | 0 | -21 | 0 |
| 1000 | 288 | 310 | 313 | 136 | 88 | 194 | 6 | -43 | 18 |
| 1500 | 479 | 495 | 480 | 242 | 166 | 294 | 27 | -58 | 0 |
| 2000 | 686 | 699 | 647 | 364 | 254 | 391 | 55 | -67 | -18 |
| 2500 | 895 | 924 | 829 | 488 | 364 | 497 | 88 | -73 | -39 |
| 3000 | 1104 | 1148 | 1006 | 627 | 479 | 585 | 134 | -73 | -61 |
| 3500 | 1320 | 1404 | 1173 | 772 | 615 | 651 | 182 | -73 | -88 |
| 4000 | 1517 | 1750 | 1364 | 933 | 812 | 663 | 237 | -61 | -167 |
| 4300 | 1626 | 1987 | | 1015 | 906 | | 270 | -67 | |
| 4400 | 1690 | | | 1066 | | | 270 | | |

TABLE 10. 27M10002 STRAIN GAGE TEST DATA (μ in./in.)

| <u>Load (lb)</u> | 1T14 | | | 2T14 | | | 3T14 | | |
|------------------|-------------|-------------|-------------|-------------|-------------|-------------|-------------|-------------|-------------|
| | <u>S/N2</u> | <u>S/N3</u> | <u>S/N4</u> | <u>S/N2</u> | <u>S/N3</u> | <u>S/N4</u> | <u>S/N2</u> | <u>S/N3</u> | <u>S/N4</u> |
| 500 | 58 | 43 | 61 | 6 | -24 | -3 | -67 | -101 | -91 |
| 1000 | 115 | 82 | 125 | 12 | -52 | -9 | -140 | -213 | -185 |
| 1500 | 173 | 122 | 185 | 12 | -82 | -18 | -225 | -323 | -282 |
| 2000 | 237 | 164 | 252 | 0 | -115 | -36 | -328 | -436 | -394 |
| 2500 | 325 | 207 | 337 | -3 | -149 | -58 | -449 | -554 | -525 |
| 3000 | 437 | 249 | 443 | -27 | -185 | -79 | -595 | -676 | -683 |
| 3500 | 562 | 304 | 580 | -45 | -218 | -109 | -758 | -816 | -880 |
| 4000 | 735 | 386 | 1069 | -85 | -264 | -400 | -998 | -993 | -1793 |
| 4300 | 947 | 465 | | -172 | -303 | | -1317 | -1145 | |
| 4400 | 1193 | | | -305 | | | -1717 | | |

TABLE 11. 27M10002 STRAIN GAGE TEST DATA ($\mu\text{in./in.}$)

| <u>Loads (lb)</u> | 1T15 | | | 2T15 | | | 3T15 | | |
|-------------------|-------------|-------------|-------------|-------------|-------------|-------------|-------------|-------------|-------------|
| | <u>S/N2</u> | <u>S/N3</u> | <u>S/N4</u> | <u>S/N2</u> | <u>S/N3</u> | <u>S/N4</u> | <u>S/N2</u> | <u>S/N3</u> | <u>S/N4</u> |
| 500 | -40 | -36 | -46 | 0 | -6 | -9 | 39 | 52 | 46 |
| 1000 | -79 | -73 | -88 | -9 | -15 | -18 | 85 | 100 | 97 |
| 1500 | -118 | -109 | -131 | -12 | -24 | -24 | 136 | 149 | 152 |
| 2000 | -161 | -143 | -176 | -18 | -30 | -27 | 191 | 197 | 212 |
| 2500 | -207 | -182 | -222 | -27 | -36 | -24 | 249 | 249 | 273 |
| 3000 | -270 | -219 | -282 | -33 | -43 | -27 | 321 | 297 | 358 |
| 3500 | -343 | -255 | -361 | -40 | -58 | -33 | 403 | 355 | 461 |
| 4000 | -452 | -306 | -723 | -36 | -82 | 155 | 522 | 421 | 958 |
| 4300 | -601 | -364 | | -9 | -112 | | 679 | 485 | |
| 4400 | -726 | | | 46 | | | 840 | | |

TABLE 12. 27M10002 COMPARISON OF TESTS AND SQ5 RESULTS ($\mu\text{in./in.}$)

Analysis at 2500 lb (before audible fiber breakage):

| | <u>SQ5</u> <u>T13</u> | <u>S/N2</u> <u>T13</u> | <u>S/N3</u> <u>T13</u> | <u>S/N4</u> <u>T13</u> |
|----------------------------|--------------------------|---------------------------|---------------------------|---------------------------|
| ϵ_x | -895 ^b | 895 | 924 | 829 |
| ϵ_y | -141 | 88 | -73 | -39 |
| γ_{xy} ^a | ± 32 | ± 7 | ± 123 | ± 204 |

a. Strain gages were not oriented consistently.

b. Probable test polarity problem. This surface is in compression.

TABLE 13. 27M10002 COMPARISON OF TEST AND SQ5 RESULTS ($\mu\text{in./in.}$)

| | SQ5 | | S/N2 | | S/N3 | | S/N4 | |
|--|-----------|---------|-----------|-----------|----------|-----------|-----------|----------|
| | T14 | T15 | T14 | T15 | T14 | T15 | T14 | T15 |
| Analysis at 2500 lb (before audible fiber damage): | | | | | | | | |
| ϵ_x | 142 | -227 | 325 | -207 | 207 | -182 | 337 | -222 |
| ϵ_y | -7 | 201 | -449 | 249 | -554 | 249 | -525 | 273 |
| γ_{xy}^a | ± 64 | ± 3 | ± 118 | ± 96 | ± 49 | ± 139 | ± 72 | ± 99 |
| Analysis at 4000 lb: | | | | | | | | |
| ϵ_x | 226 | -363 | 735 | -452 | 386 | -306 | 1069 | -723 |
| ϵ_y | -11 | 322 | -998 | 522 | -993 | 421 | -1763 | 958 |
| γ_{xy}^a | ± 103 | ± 5 | ± 93 | ± 142 | ± 79 | ± 279 | ± 106 | ± 75 |

a. Strain gages were not oriented consistently.

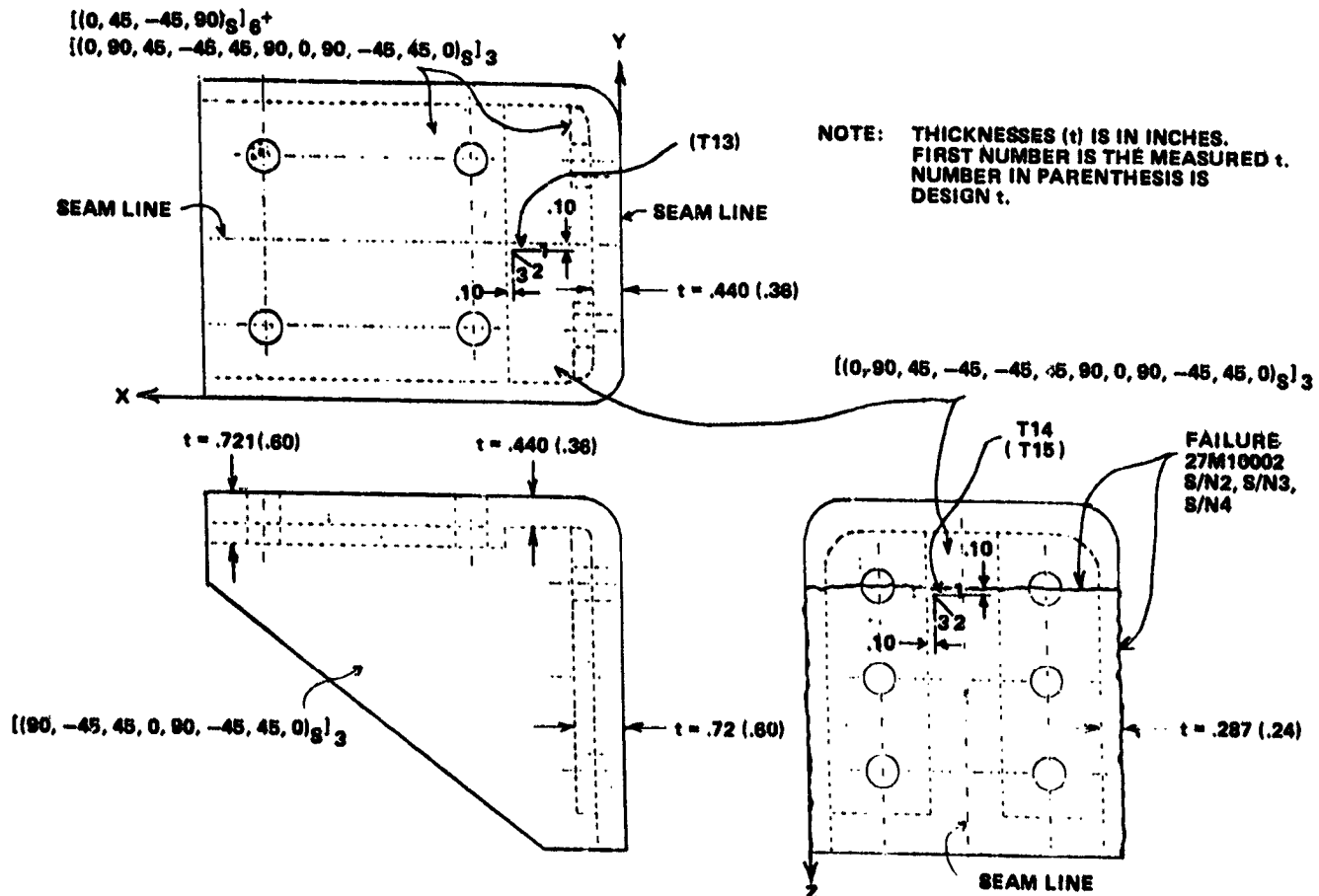


Figure 12. Strain gage and failure locations.

3. 27M10003 Test Results

Tables 14 through 16 present strain gage test data. Tables 17 and 18 present comparison of test and analytical results. Locations of strain gages are presented on Figure 13. S/N2 and S/N3 failed across the bolt holes on the x-face at an average load of 3463 lb. S/N1 was not retrofitted with a radius insert and failed across the bolt holes and stiffener on the z-face at a load of 2229 lb.

TABLE 14. 27M10003-STRAIN GAGE TEST DATA (μ in./in.)

| Load (lb) | 1T13 | | | 2T13 | | | 3T13 | | |
|-----------|-------------------|------|------|-------------------|------|------|-------------------|------|------|
| | S/N1 ^a | S/N2 | S/N3 | S/N1 ^a | S/N2 | S/N3 | S/N1 ^a | S/N2 | S/N3 |
| 500 | 273 | 158 | 79 | 239 | 118 | 27 | 94 | 9 | -6 |
| 1000 | 526 | 337 | 152 | 430 | 248 | 49 | 152 | 30 | -12 |
| 1500 | 1015 | 550 | 246 | 763 | 400 | 79 | 137 | 55 | -9 |
| 2000 | 1938 | 796 | 355 | 1387 | 585 | 128 | -58 | 91 | -3 |
| 2500 | | 1057 | 504 | | 806 | 222 | | 134 | 21 |
| 3000 | | 1340 | 717 | | 993 | 383 | | 176 | 64 |
| 3100 | | 1410 | 760 | | 1057 | 434 | | 188 | 82 |
| 3200 | | 1571 | 811 | | 1157 | 483 | | 179 | 88 |
| 3500 | | | 963 | | | 635 | | | 125 |
| 3600 | | | 1030 | | | 757 | | | 131 |

a. Did not have radius insert

TABLE 15. 27M10003 STRAIN GAGE TEST DATA (μ in./in.)

| Load (lb) | 1T14 | | | 2T14 | | | 3T14 | | |
|-----------|-------------------|------|------|-------------------|------|------|-------------------|-------|-------|
| | S/N1 ^a | S/N2 | S/N3 | S/N1 ^a | S/N2 | S/N3 | S/N1 ^a | S/N2 | S/N3 |
| 500 | 82 | 55 | 46 | -12 | -43 | -40 | -116 | -125 | -113 |
| 1000 | 164 | 109 | 91 | -30 | -97 | -88 | -238 | -268 | -235 |
| 1500 | 270 | 167 | 137 | -55 | -152 | -143 | -375 | -414 | -369 |
| 2000 | 389 | 231 | 188 | -112 | -209 | -201 | -536 | -576 | -512 |
| 2500 | | 307 | 243 | | -255 | -256 | | -737 | -664 |
| 3000 | | 465 | 316 | | -291 | -304 | | -1045 | -832 |
| 3100 | | 525 | 337 | | -328 | -310 | | -1185 | -871 |
| 3200 | | 598 | 352 | | -358 | -316 | | -1401 | -908 |
| 3500 | | | 416 | | | -344 | | | -1026 |
| 3600 | | | 459 | | | -411 | | | -1167 |

a. Did not have radius insert.

TABLE 16. ...27M10003 STRAIN GAGE TEST DATA ($\mu\text{in./in.}$)

| Load (lb) | 1T15 | | | 2T15 | | | 3T15 | | |
|-----------|-------------------|------|------|-------------------|------|------|-------------------|------|------|
| | S/N1 ^a | S/N2 | S/N3 | S/N1 ^a | S/N2 | S/N3 | S/N1 ^a | S/N2 | S/N3 |
| 500 | -52 | -46 | -58 | 0 | 6 | 3 | 76 | 70 | 67 |
| 1000 | -106 | -97 | -118 | 9 | 12 | 9 | 155 | 140 | 133 |
| 1500 | -179 | -149 | -185 | 21 | 27 | 18 | 237 | 215 | 212 |
| 2000 | -243 | -203 | -246 | 55 | 40 | 30 | 309 | 297 | 297 |
| 2500 | | -258 | -304 | | 36 | 46 | | 382 | 391 |
| 3000 | | -367 | -370 | | 6 | 61 | | 531 | 503 |
| 3100 | | -392 | -383 | | 30 | 61 | | 588 | 525 |
| 3200 | | -410 | -398 | | 52 | 61 | | 676 | 546 |
| 3500 | | | -437 | | | 67 | | | 619 |
| 3600 | | | -577 | | | 161 | | | 940 |

a. Did not have radius insert.

TABLE 17. 27M10003 COMPARISON OF TEST AND SQ5 RESULTS ($\mu\text{in./in.}$)

| | SQ5 T13 | S/N1 ^a T13 | S/N2 T13 | S/N3 T13 |
|----------------------------|-------------------|--------------------------|-------------|-------------|
| ϵ_x | -353 ^c | 526 | 337 | 152 |
| ϵ_y | -46 | 152 | 30 | -12 |
| γ_{xy} ^b | ± 12 | ± 182 | ± 129 | ± 42 |

- a. Did not have radius insert.
- b. Strain gages were not oriented consistently.
- c. Probable test polarity problem. This surface is in compression.

TABLE 18. 27M10003. COMPARISON OF TEST AND SQ5 RESULTS ($\mu\text{in./in.}$)

| | SQ5 | | S/N1 ^a | | S/N2 | | S/N3 | |
|--|----------|----------|-------------------|----------|----------|----------|----------|---------|
| | T14 | T15 | T14 | T15 | T14 | T15 | T14 | T15 |
| Analysis at 1000 lb (before audible fiber breakage): | | | | | | | | |
| ϵ_x | 72 | -121 | 164 | -106 | 109 | -97 | 91 | -118 |
| ϵ_y | -36 | 106 | -238 | 155 | -268 | 140 | -235 | 133 |
| γ_{xy} ^b | ± 34 | ± 11 | ± 14 | ± 31 | ± 35 | ± 19 | ± 32 | ± 3 |
| Analysis at 2500 lb: | | | | | | | | |
| ϵ_x | 179 | -304 | | | 307 | -258 | 243 | -304 |
| ϵ_y | -91 | 265 | | | -737 | 382 | -664 | 392 |
| γ_{xy} ^b | ± 84 | ± 28 | | | ± 80 | ± 52 | ± 91 | ± 4 |

- a. Did not have radius insert.
- b. Strain gages were not oriented consistently.

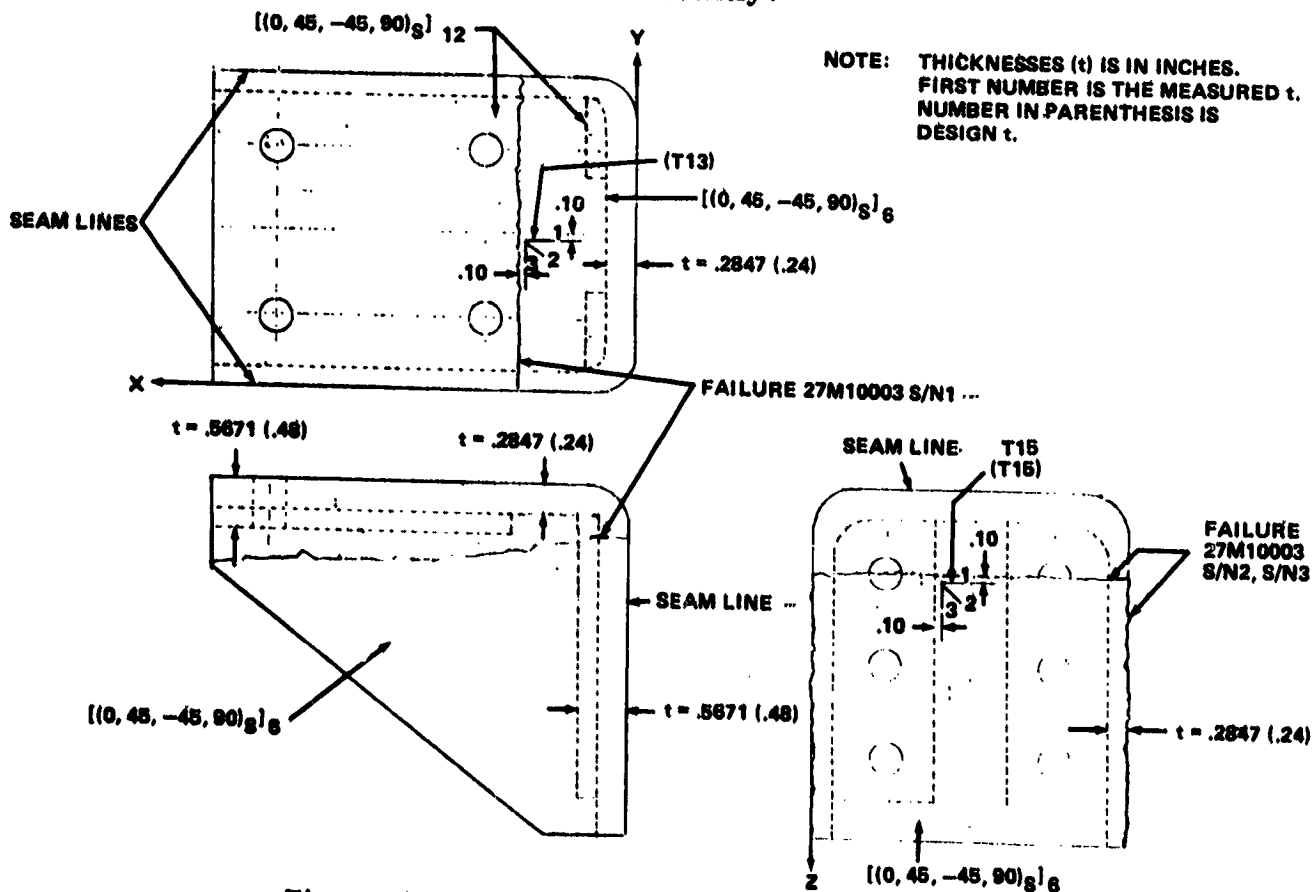


Figure 13. Strain gage and failure locations.

4. 27M10009 Test Results

Tables 19 through 21 present strain gage test data. Tables 22 and 23 present comparison of test and analytical results. Locations of strain gages are presented on Figure 14. The fittings were made by bonding three laminated pieces together with Hysol EA-934. The two fittings failed along the bond lines at an average load of 3126 lb. Hysol EA-934 has an ultimate shear strength of 3100 psi. However, based on the bonding area of the sides (y-face) alone, the bond failed at 143 psi.

TABLE 19. 27M10009 STRAIN GAGE TEST DATA (μ in./in.)

| <u>Load (lb)</u> | 1T13 | | 2T13 | | 3T13 | |
|------------------|-------------|-------------|-------------|-------------|-------------|-------------|
| | <u>S/N1</u> | <u>S/N2</u> | <u>S/N1</u> | <u>S/N2</u> | <u>S/N1</u> | <u>S/N2</u> |
| 500 | 94 | 33 | 106 | 15 | 47 | 15 |
| 1000 | 204 | 119 | 228 | 61 | 106 | 46 |
| 1500 | 334 | 267 | 368 | 158 | 191 | 115 |
| 2000 | 456 | 428 | 513 | 273 | 295 | 213 |
| 2500 | 556 | 529 | 647 | 346 | 401 | 322 |
| 3000 | 842 | 817 | 936 | 535 | 783 | 519 |
| 3100 | | 939 | | 611 | | 586 |
| 3200 | | 1109 | | 720 | | 686 |

TABLE 20. 27M10009 STRAIN GAGE TEST DATA (μ in./in.)

| <u>Load (lb)</u> | 1T14 | | 2T14 | | 3T14 | |
|------------------|-------------|-------------|-------------|-------------|-------------|-------------|
| | <u>S/N1</u> | <u>S/N2</u> | <u>S/N1</u> | <u>S/N2</u> | <u>S/N1</u> | <u>S/N2</u> |
| 500 | 43 | 36 | 9 | 9 | -46 | -34 |
| 1000 | 85 | 73 | 21 | 18 | -94 | -67 |
| 1500 | 137 | 118 | 30 | 30 | -146 | -110 |
| 2000 | 182 | 167 | 37 | 34 | -107 | -165 |
| 2500 | 231 | 213 | 21 | -91 | -289 | -423 |
| 3000 | 143 | 131 | -280 | -335 | -664 | -691 |
| 3100 | | 134 | | -374 | | -755 |
| 3200 | | 140 | | -475 | | -899 |

TABLE 21. 27M10009 STRAIN GAGE TEST DATA ($\mu\text{in./in.}$)

| Loads (lb) | 1T15 | | 2T15 | | 3T15 | |
|------------|------|------|------|------|------|------|
| | S/N1 | S/N2 | S/N1 | S/N2 | S/N1 | S/N2 |
| 500 | -30 | -24 | -6 | 0 | 34 | 27 |
| 1000 | -64 | -55 | -12 | 3 | 67 | 49 |
| 1500 | -100 | -85 | -21 | -12 | 103 | 70 |
| 2000 | -140 | -118 | -27 | -18 | 143 | 97 |
| 2500 | -182 | -161 | -24 | -55 | 192 | 125 |
| 3000 | -240 | -197 | 210 | 67 | 612 | 313 |
| 3100 | | -213 | | 55 | | 341 |
| 3200 | | -252 | | 46 | | 414 |

TABLE 22. 27M10009 COMPARISON OF TEST AND SQ5 RESULTS ($\mu\text{in./in.}$)

Analysis at 1500 lb. (before audible fiber breakage):

| | SQ5 T13 | S/N1 T13 | S/N2 T13 |
|----------------------------|-------------------|-----------|----------|
| ϵ_x | -368 ^b | 334 | 267 |
| ϵ_y | -138 | 191 | 115 |
| γ_{xy} ^a | ± 59 | ± 211 | ± 66 |

- a. Strain gages were not oriented consistently.
 b. Probable test polarity problem. This surface is in compression.

TABLE 23. 27M10009 COMPARISON OF TEST AND SQ5 RESULTS ($\mu\text{in./in.}$)

| | SQ5 | | S/N1 | | S/N2 | |
|----------------------------|----------|----------|----------|----------|----------|---------|
| | T14 | T15 | T14 | T15 | T14 | T15 |
| ϵ_x | 206 | -25 | 137 | -100 | 118 | -85 |
| ϵ_y | -138 | 66 | -146 | 103 | -110 | 70 |
| γ_{xy} ^a | ± 19 | ± 34 | ± 69 | ± 45 | ± 52 | ± 9 |

- a. Strain gages were not oriented consistently.

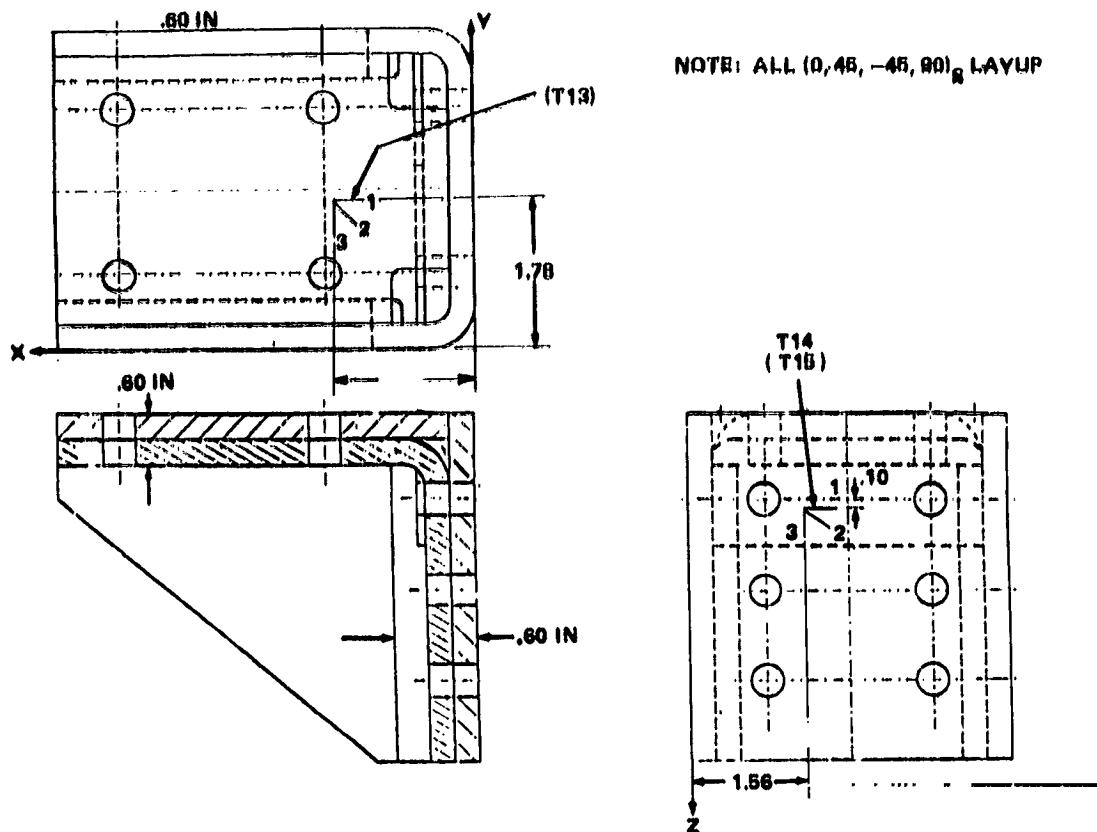


Figure 14. Strain gage locations.

CONCLUSIONS AND RECOMMENDATIONS

27M10001, 27M10002, and 27M10003 are similar in design except for layup and seam locations. As can be concluded from the ultimate failure loads, thickness was the most important factor with 27M10002 being the thickest and strongest of the three designs. When the laminate is quasi-isotropic and balanced, thickness will determine ultimate load capability.

27M10009 failed at the lowest load even though it was the thickest of all four designs. Bonding three sections together with Hysol EA-934 was not a good design. However, this could also have resulted from faulty fabrication.

The test results did not closely correlate with the analytical results. Test results between the fittings of each configuration did not closely correlate either. The lack of correlation within a given configuration is probably due to the lack of good quality control in the fabrication process. However, this type of variation is inherent in composites.

EP42 does not have the analysis capability to redistribute loads if one or more lamina fails prior to gross failure of the laminate. Both SPAR and SQ5 perform linear analysis. The overall behavior of the laminate is nonlinear if one or more lamina fails prior to gross laminate failure. To perform adequate analysis, a 3-D finite element program that performs progressive failure analysis is required. Such a progressive failure analysis is presented in Figure 15.

ORIGINAL PAGE IS
OF POOR QUALITY.

Several problems were encountered. On the first component, the application of a kapton backing between the strain gages and the part proved very time consuming and also resulted in gage problems. The backing was eliminated for the other components. Application of gages was performed by the different groups, which negated the learning curves in applying the devices. Due to scheduling problems, the initial sequence between tests, namely a two-week spacing for data reduction and correlation, and strain gage location determination, was not maintained. Strain gage location on subsequent components were determined without the benefit of previous test results. Finally, there was the change in thickness of the fabricated parts, as mentioned before. As large variation of thickness was encountered, it made the data reduction, reanalysis and correlation between like components difficult. The same problems were present on the plate material used for material property evaluation. Even so, the obtained values appeared reasonable, accuracy could have been improved by using more time and more sample materials. A certain thickness dependence of the properties was observed in the quasi-isotropic layup, which would require additional work in the future. In general, the development program showed the need for additional experimental and analytical effort in the event of composite use for complex fittings and shapes.

Macromechanical Behavior of a Laminate - 194.

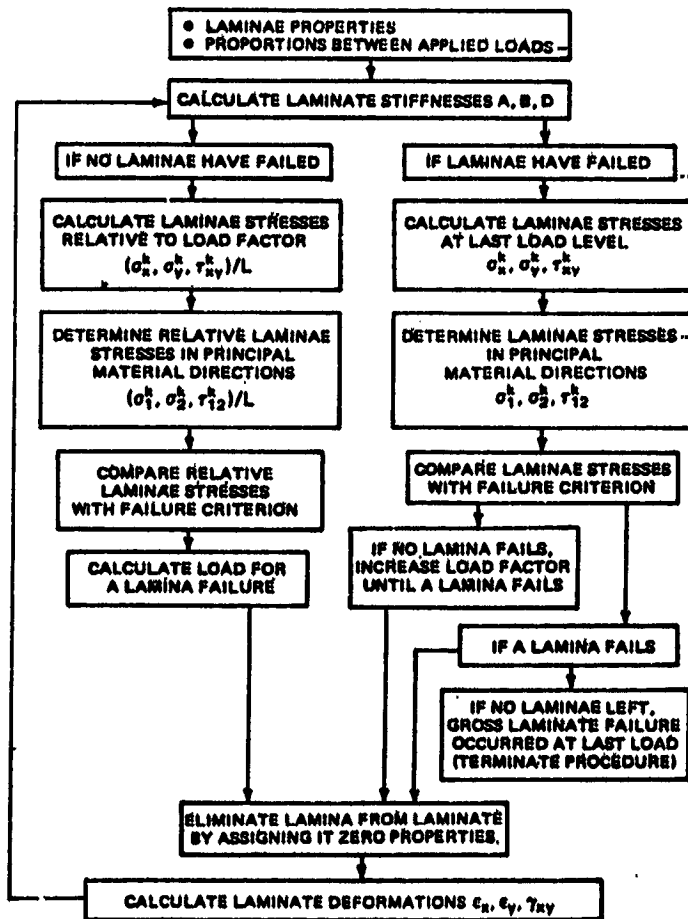


FIG. 4-24. Analysis of laminate strength and load-deformation behavior.

* Ref: Jones, Robert M., Mechanics of Composite Materials, 1975

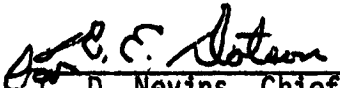
Figure 15. Progressive failure analysis.

APPROVAL


DEVELOPMENT AND TEST OF ADVANCED COMPOSITE COMPONENTS

By G. Faile, R. Hollis, F. Ledbetter, J. Maldonado, J. Sledd,
J. Stuckey, G. Waggoner, and E. Engler

The information in this report has been reviewed for technical content. Review of any information concerning Department of Defense or nuclear energy activities or programs has been made by the MSFC Security Classification Officer. This report, in its entirety, has been determined to be unclassified.


C. D. Nevins, Chief
Structures Division


P. W. Frederick, Chief
Engineering Analysis Division


A. A. McCool, Director
Structures and Propulsion Laboratory